Effects of Different Silt Particle Concentrations on Cavitation Evolution in the Centrifugal Pump

Xiangdong Han[1], Youchao Yang[2], Chao Wang[2], Weiguo Zhao[3], and Pengjun Fan[4(✉)]

[1] School of Civil Engineering, Nanchang Institute of Technology, Nanchang 330044, China
[2] Chongqing Pump Industry Co., Ltd., Chongqing 400033, China
[3] College of Energy and Power Engineering, Lanzhou University of Technology, Lanzhou 730050, China
[4] Machine Industry Lanzhou Petrochemical Equipment Inspection Institute Co., LTD., Lanzhou 730070, China
fanpengjun@lanpec.com

Abstract. Numerical simulations on effects of diverse silt particle concentrations on cavitation evolution in the centrifugal pump were performed. It was silt particle-water cavitation flow. The concentrations employed were 1%, 5%, and 10%. Evolutions of cavitation bubbles and streamlines and variations of head were studied. Results indicated that under the cavitation number of 0.55, cavitation evolution degree under the concentration of 1% became stronger than in pure water cavitation flow (PWCF); for 5% and 10%, the degrees were weaker than that of PWCF. Streamlines were more disorder and corresponding regions were larger for 1% and 10%; for 5%, they had contrary variations. Head increased first and then, decreased. At the cavitation number of 0.11, cavitation evolution degree under all concentration conditions were more intense than in PWCF. With the concentration increase, cavitation evolution degree was stronger; streamline disorder degree was more intense and corresponding regions were larger; head decreased steadily.

Keywords: Silt particle-water cavitation flow · Silt particle concentration · Centrifugal pump · Numerical simulation

1 Introduction

Hydraulic machinery, such as centrifugal pump and hydro turbine, which operates in rivers with silt particles and suspended sediments [1], is confronted with the synergetic destruction of cavitation erosion (CE) and silt particle abrasion (SPA) [2]. The internal flow is silt particle-water cavitation flow (SPWCF), one kind of solid-liquid-vapor three-phase flow with mass transfer and phase change [3], different from pure water cavitation flow (PWCF) [4].

Some scholars investigated the combined destruction of CE and SPA. Jin et al. [5] discussed effects of particles on the characteristics of CE in one hydraulic turbine. The joint destruction was much severer than the single action of CE or SPA. Gou et al. [6] employed the magnetostriction apparatus to experimentally discuss effects of particles

L. Yan and J. Na (Eds.): ICFPMCE 2022, AHE 10, pp. 282–290, 2023.
https://doi.org/10.2991/978-94-6463-022-0_25

with various densities and diameters on the joint destruction of CE and SPA of 1045 carbon steel. The meaningful conclusion they obtained was that under diverse conditions, laws of variation of the synergetic destruction of CE and SPA were different. Madadnia et al. [7] got that in particle-laden cavitation flow, cavitation erosion on the material surface was accelerated. Chen et al. [8] performed vibration cavitation erosion experiments to determine the effects of particles with five different sizes. The results indicated that particles with the diameter of 500 nm could induce the severest destruction.

For our present study, effects of silt particles with different concentrations on cavitation evolution under different cavitation numbers were analyzed. The concentrations were 1%, 5%, and 10%. Distributions of cavitation bubbles and streamlines and variations of head were discussed.

2 Numerical Simulation Method

2.1 Fundamental Equations

The employed continuous equation, momentum equation, transportation equations for vapor and silt particles, and relative velocity equation of the numerical simulation of SPWCF are shown as follows [9]. Mass transfer caused by cavitation occurred between water with vapor; for silt particles, this process was not considered. Water was taken as the principal phase; for vapor and silt particles, they were the secondary phase. Water and vapor were continuous media and they had the identical pressure and velocity fields. Silt particles were generally the discrete medium; due to the small mean diameters, they were regarded as the pseudo-fluid.

$$\frac{\partial \rho_{\mathrm{m}}}{\partial t} + \frac{\partial \left(\rho_{\mathrm{m}} u_j\right)}{\partial x_j} = 0 \tag{1}$$

$$\frac{\partial (\rho_{\mathrm{m}} u_i)}{\partial t} + \frac{\partial \left(\rho_{\mathrm{m}} u_i u_j\right)}{\partial x_j} = -\frac{\partial p}{\partial x_i} + \frac{\partial}{\partial x_j}\left(\mu_{\mathrm{m}} \frac{\partial u_i}{\partial x_j}\right) \tag{2}$$

$$\frac{\partial \rho_{\mathrm{v}} \alpha_{\mathrm{v}}}{\partial t} + \frac{\partial \left(\rho_{\mathrm{v}} \alpha_{\mathrm{v}} u_j\right)}{\partial x_j} = m_{\mathrm{c}} - m_{\mathrm{e}} \tag{3}$$

$$\frac{\partial \rho_{\mathrm{s}} \alpha_{\mathrm{s}}}{\partial t} + \frac{\partial \left(\rho_{\mathrm{s}} \alpha_{\mathrm{s}} u_j\right)}{\partial x_j} = 0 \tag{4}$$

$$\mathbf{v}_{\mathrm{pq}} = \mathbf{v}_{\mathrm{p}} - \mathbf{v}_{\mathrm{q}} \tag{5}$$

where ρ_{m} is the mixture density and u is the mixture velocity. x is coordinate. t is time. i and j are subscripts. p is pressure. μ_{m} is mixture viscosity. ρ_{v} is the density of vapor, and ρ_{s} is the density of silt particles. α_{v} and α_{s} are volume fractions of vapor and silt particles, respectively. m_{e} and m_{c} are source terms of evaporization and condensation. $\mathbf{V}_{\mathrm{pq}}$ is relative velocity vector between primary phase with secondary phase. $\mathbf{V}_{\mathrm{p}}$ is primary phase velocity vector; in SPWCF, it is the water velocity vector. $\mathbf{V}_{\mathrm{q}}$ is secondary phase velocity vector; they are the velocity vectors of vapor and silt particles.

2.2 Turbulence Model

SST k-ω turbulence model [10] was used to solve the turbulent flow in this centrifugal pump. It integrated the merits of k-ε models and standard k-ω model; therefore, it was particularly robust. Turbulent kinetic energy equation and specific dissipation rate equation are as follows:

$$\rho_{\mathrm{m}}\frac{\partial k}{\partial t}+\rho_{\mathrm{m}}\overline{u_j}\frac{\partial k}{\partial x_j}=P_k-\rho_{\mathrm{m}}\beta_*\omega k+\frac{\partial}{\partial x_j}\left[\left(\mu+\frac{\mu_{\mathrm{t}}}{\sigma_k}\right)\frac{\partial k}{\partial x_j}\right] \tag{6}$$

$$\begin{aligned}\rho_{\mathrm{m}}\frac{\partial \omega}{\partial t}+\rho_{\mathrm{m}}\overline{u_j}\frac{\partial \omega}{\partial x_j}=&\alpha P_\omega-\rho_{\mathrm{m}}\beta_*\omega^2+\frac{\partial}{\partial x_j}\left[\left(\mu+\frac{\mu_{\mathrm{t}}}{\sigma_\omega}\right)\frac{\partial \omega}{\partial x_j}\right]\\&+2\rho_{\mathrm{m}}(1-F_1)\frac{1}{\sigma_{\omega_{\mathrm{out}}}\omega}\frac{\partial k}{\partial x_j}\frac{\partial \omega}{\partial x_j}\end{aligned} \tag{7}$$

where k is turbulent kinetic energy and ω is specific dissipation rate. P_k and P_ω are the corresponding production terms. μ_{tur} is turbulent viscosity and μ is dynamic viscosity. F_1 is one blending function. σ_k and σ_ω are empirical coefficients. $\sigma_{\omega\mathrm{out}}$ and β_* are taken as 1.168 and 0.09.

Similar with the modification on turbulent viscosity in RNG k-ε turbulence model [11], the viscosity in SST k-ω turbulence model was modified.

2.3 Cavitation Model

Cavitation model proposed by Zwart, Gerber, and Belamri was employed to numerically simulate the mass transfer and phase change for SPWCF in the centrifugal pump [12]. The evaporization and condensation source terms are as follows:

$$m_{\mathrm{e}}=F_{\mathrm{vap}}\frac{3\alpha_{\mathrm{nuc}}(1-\alpha_{\mathrm{v}})\rho_{\mathrm{v}}}{r_{\mathrm{b}}}\sqrt{\frac{2}{3}\frac{p_{\mathrm{v}}-p}{\rho_{\mathrm{l}}}} \tag{8}$$

$$m_{\mathrm{c}}=F_{\mathrm{cond}}\frac{3\alpha_{\mathrm{v}}\rho_{\mathrm{v}}}{r_{\mathrm{b}}}\sqrt{\frac{2}{3}\frac{p-p_{\mathrm{v}}}{\rho_{\mathrm{l}}}} \tag{9}$$

where α_{nuc} is the volume fraction of nucleation site. r_{b} is cavitation bubble radius. p_{v} is saturated vapor pressure. F_{vap} and F_{cond} are empirical constants, taken as 50 and 0.01, respectively.

3 Numerical Simulation Setup

3.1 Physical Model

One centrifugal pump was employed to perform the numerical simulation of SPWCF. The model included impeller, volute, suction pipe, and exit pipe.

Main performance parameters were that designed flow rate $Q_{\mathrm{d}}=25.8\ \mathrm{m}^3/\mathrm{h}$, design head $H_{\mathrm{d}}=38.5$, efficiency $\eta=42\%$, rotational speed $n=1460$ r/min, and specific speed $n_{\mathrm{s}}=32$.

Primary geometrical parameters for the impeller included inlet diameter $D_j=90$ mm, outlet diameter $D_2=65$ mm, inlet angle $\beta_1=37°$, outlet angle $\beta_2=37°$, outlet width $b_2=12$ mm, and blade number $Z=6$ (Fig. 1).

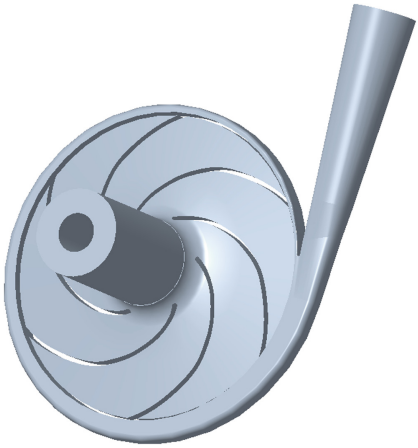

Fig. 1. Centrifugal pump computational domain.

Fig. 2. Meshes of the centrifugal pump.

3.2 Mesh Generation

ANSYS-ICEM (Version: 2022R1) was used to generate the meshes. For suction pipe and impeller, hexahedral structured meshes were utilized to discretize the computational domains; the numbers were 925106 and 1286850. For the ensemble of volute and exit pipe, they were tetrahedral unstructured meshes; the number was 857931. For the centrifugal pump, the total number was 3069887 (Fig. 2).

3.3 Material Properties and Boundary Conditions

In the numerical simulation process, water density was $\rho_l = 998.2\,\text{kg/m}^3$ and the dynamic viscosity was $\mu_l = 0.001\,\text{kg/m} \cdot \text{s}$. For vapor, they were $0.02558\,\text{kg/m}^3$ and 1.26×10^{-6} kg/m·s. Saturated vapor pressure was $P_v = 3540$ Pa. Density of silt particles was $\rho_s = 2650\,\text{kg/m}^3$.

At inlet, it was set as total pressure; for outlet, it was mass flow rate. The operation pressure was 0Pa. Volume fraction of water at inlet was 1 and for vapor, it was 0. Transient frozen rotor was set in the rotor-stator interface. Time step was $\Delta t = 3.34 \times 10^{-4}$s, which was the time of every 3° rotation for the impeller. Total time was 0.2 s.

4 Results and Discussion

Silt particle mean diameter was 0.025 mm. Silt particle concentrations were taken as 1%, 5%, and 10% to investigate its effects on cavitation evolution in this centrifugal pump.

Cavitation number for the centrifugal pump was defined in the following equation [13]; for our numerical simulation, the values were 0.55 and 0.11.

$$\sigma = \frac{p - p_{\mathrm{v}}}{\frac{1}{2}\rho_{\mathrm{l}} v^2} \tag{10}$$

where σ is cavitation number. v is centrifugal pump inlet velocity, which is given as:

$$u = \frac{n\pi D_1}{60} \tag{11}$$

For the head, it was calculated as:

$$H = \frac{P_{\mathrm{out}} - P_{\mathrm{in}}}{\rho_{\mathrm{l}} g} \tag{12}$$

where H is head. P_{out} and P_{in} are respectively the total pressure for outlet and inlet.

Distributions of cavitation bubbles with $\alpha_{\mathrm{v}} = 0.1$ and streamlines in the impeller under $\sigma = 0.55$ are shown in Fig. 3. Cavitation bubbles were mainly concentrated at the inlet of back surfaces. For the vortices, they were filled in the flow passages.

In PWCF, the calculated head was 42.27 m. Under $\alpha_{\mathrm{s}} = 1\%$, cavitation bubbles became more; therefore, cavitation development degree became stronger. Streamlines were more disorder and corresponding distribution regions of vortices became larger; under their effects, the head was smaller; it was 42.21 m. For $\alpha_{\mathrm{s}} = 5\%$, cavitation bubbles were fewer; the development degree was weaker than in PWCF. On the other hand, compared with PWCF, the disorder degree of streamlines was weaker and the regions for vortices became smaller. The head was 42.29 m. At $\alpha_{\mathrm{s}} = 10\%$, the bubbles were fewer than those of PWCF. The evolution degree was weaker than in PWCF. Streamlines were more disorder and distribution regions of vortices became larger. The head was 42.23 m (Fig. 4).

Figure 5 is the distributions of cavitation bubbles and streamlines under $\sigma = 0.11$. Compared with $\sigma = 0.55$, cavitation bubbles became more. Furthermore, streamlines were more disorder and distribution regions of vortices became larger. At $\sigma = 0.11$, cavitation had particularly significant development. With the increase of silt particle concentration, the bubbles were more. Also, disorder degree of streamlines was more intense and distribution regions of vortices became larger. For the head under PWCF condition, it was 41.23 m. In SPWCF with $\alpha_{\mathrm{s}} = 1\%$, the head calculated was 41.11 m. Under $\alpha_{\mathrm{s}} = 5\%$ and 10%, they were 41.04 m and 40.55 m (Fig. 6).

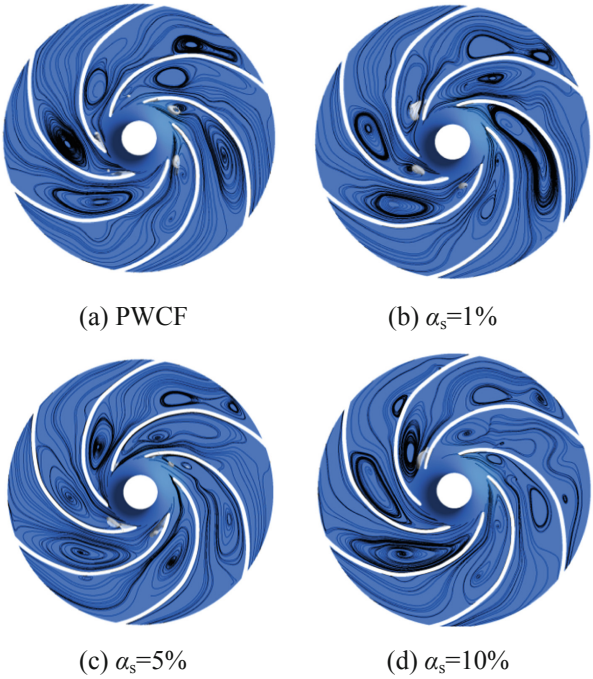

(a) PWCF (b) α_s=1%

(c) α_s=5% (d) α_s=10%

Fig. 3. Distributions of cavitation bubbles and streamlines under $\sigma = 0.55$.

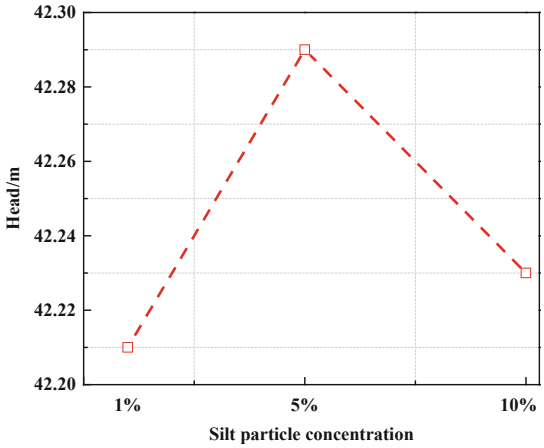

Fig. 4. Variations of head with silt particle concentration under $\sigma = 0.55$.

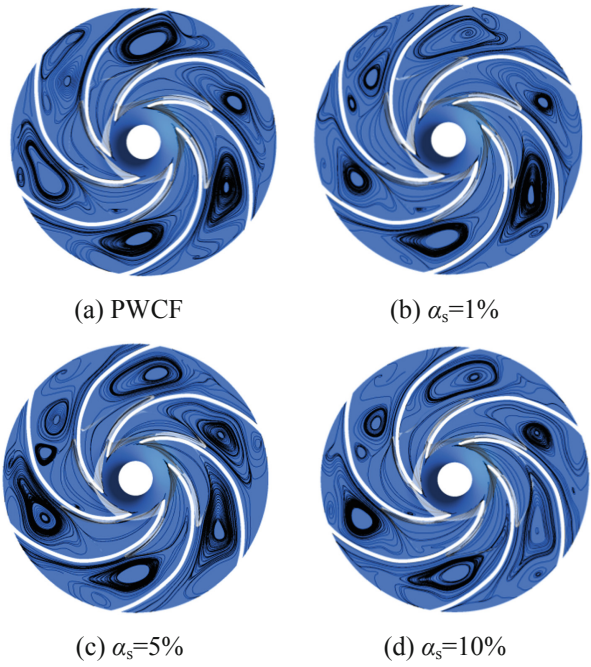

Fig. 5. Distributions of cavitation bubbles and streamlines under $\sigma = 0.11$.

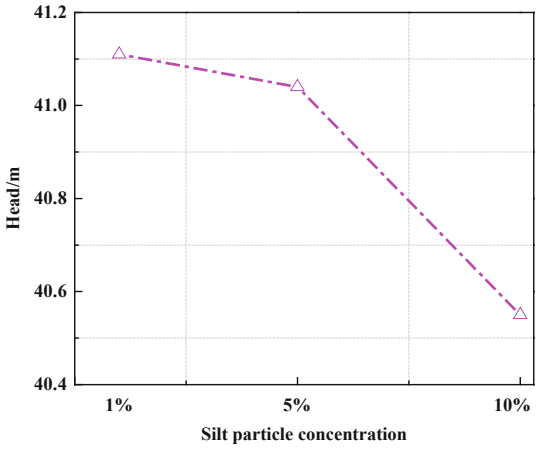

Fig. 6. Variations of head with silt particle concentration under $\sigma = 0.11$.

5 Conclusions

Numerical simulations of SPWCF with the concentrations of 1%, 5%, and 10% in the centrifugal pump under the cavitation numbers of 0.55 and 0.11 were performed. Variations of cavitation bubbles, streamlines, and head were discussed. Primary conclusions were as follows:

(1) Cavitation evolution degree for the cavitation number of 0.11 under the concentration of 1% in SPWCF was stronger than in PWCF. Streamlines were more disorder and distribution regions of vortices were larger. The head was 42.21 m. For 5%, all laws of variation were contrary to that of 1%. The head was 42.29 m. At 10%, the evolution degree was weaker than that of PWCF; streamline disorder degree was more intense and corresponding regions were larger. The head was 42.23 m.
(2) With the increase of the concentration, cavitation evolution degree became stronger steadily and they were all more intense than in PWCF. Streamlines were more disorder and the distribution regions became larger. The head was 41.11 m, 41.04 m, and 40.05 m.

Acknowledgments. The investigation was financially supported by National Natural Science Foundation of China (Grant No. 52169018).

References

1. Peker, S.M., Helvaci, S.S.: Solid-Liquid Two Phase Flow. Elsevier Science (2007)
2. Zhao, W.G., Han, X.D., Li, R.N., Zheng, Y.J., Wang, Y.Y.: Effects of size and concentration of silt particles on flow and performance of a centrifugal pump under cavitating conditions. Mod. Phys. Lett. B **31**(34), 1750312 (2017). https://doi.org/10.1142/S0217984917503122
3. Han, X.D., Kang, Y., Zhao, W.G., Sheng, J.P., Li, D.: Silt particles affect cavitation flow: analyzing variations in silt mean diameter and concentration. Powder Technol. **356**, 671–690 (2019). https://doi.org/10.1016/j.powtec.2019.09.005
4. Ghadimi, A., Ghassemi, H.: Comparative assessment of hydrodynamic performance of two-dimensional Naca0012 and Naca6612 hydrofoils under different cavitation and non-cavitation conditions. Int. J. Hydromechatronics **3**(4), 349–367 (2020). https://doi.org/10.1504/IJHM.2020.112161
5. Jin, H.Y., Zheng, F.Z., Li, S.Y., Hang, C.Z.: The role of sand particles on the rapid destruction of the cavitation zone of hydraulic turbines. Wear **112**(2), 199–205 (1986). https://doi.org/10.1016/0043-1648(86)90240-1
6. Gou, W.J., Zhang, H., Li, H.P., Liu, F., Lian, J.J.: Effects of silica sand on synergistic erosion caused by cavitation, abrasion, and corrosion. Wear **412–413**, 120–126 (2018). https://doi.org/10.1016/j.wear.2018.07.023
7. Madadnia, J., Owen, I.: Accelerated surface erosion by cavitating particulate-laden flows. Wear **165**(1), 113–126 (1993). https://doi.org/10.1016/0043-1648(93)90380-5
8. Chen, H.S., Liu, S.H., Wang, J.D., Chen, D.R.: Study on effect of microparticle's size on cavitation erosion in solid-liquid system. J. Appl. Phys. **101**, 103510 (2007). https://doi.org/10.1063/1.2734547

9. Sharma, A.: Introduction to Computational Fluid Dynamics: Development, Application and Analysis, Springer, Cham (2021). https://doi.org/10.1007/978-3-030-72884-7
10. Wilcox, D.C.: Simulation of transition with a two-equation turbulence model. AIAA J. **32**(2), 247–255 (1994). https://doi.org/10.2514/3.59994
11. Coutier-Delgosha, O., Stutz, B., Vabre, A., Legoupil, S.: Analysis of cavitating flow structure by experimental and numerical investigations. J. Fluid Mech. **578**, 171–222 (2007). https://doi.org/10.1017/S0022112007004934
12. Zwart, P.J., Gerber, A.G., Belamri, T.: A two-phase flow model for predicting cavitation dynamics. In: Proceedings of ICMF 2004 International Conference on Multiphase Flow, Yokohama, Japan (2004)
13. Zaher, M.A.: Centrifugal Pump Technology and Pump Cavitation. Createspace Independent Publishing Platform (2015)